The Journal of the Korean Society of
Coastal and Ocean Engineers
Vol. 6, No. 2, pp. 139~149, June 1994

Infinite Element for the Analysis of Harbor Resonances
港灣 副振動 解析을 위한 無限要素

Woo Sun Park*, In Sik Chun* and Weon Mu Jeong*
朴佑善* · 全仁植* · 鄭遠武*

Abstract □ In this paper, a finite element technique is applied to the prediction of the wave resonance phenomena in harbors. The mild-slope equation is used with a partial reflection boundary condition introduced to model the energy dissipating effects on the solid boundary. For an efficient modeling of the radiation condition at infinity, a new infinite element is developed. The shape function of the infinite element is derived from the asymptotic behavior of the first kind of the Hankel's function in the analytical boundary series solutions. For the computational efficiency, the system matrices of the element are constructed by performing the relevant integrations in the infinite direction analytically. Comparisons with the results from experiments and other solution methods show that the present model gives fairly good results. Numerical experiments are also carried out to determine the proper distance to the infinite elements from the mouth of the harbor, which directly affect the accuracy and efficiency of the solution.

要 旨 : 本 論文에서는 港灣 副振動現像을 豫測할 수 있는 無限要素를 이용한 有限要素技法에 대해서 硏究하였다. 支配方程式으로는 緩傾斜方程式을 사용하였으며, 固體境界面에서의 에너지 損失效果를 고려하기 위하여 部分反射條件을 導入하였다. 外部領域 無限境界條件을 效率的으로 處理하기 위하여 새로운 無限要素를 개발하였다. 개발된 無限要素의 形象函數는 解析的 固有函數의 級數解의 進行波項을 나타내는 제 1종 Hankel 函數의 漸近的 形態를 사용하여 결정하였다. 數値解析上의 效率性을 提高하기 위하여 無限要素의 시스템행렬 構成시 나타나는 無限方向으로의 積分을 解析的으로 수행하였다. 旣存의 數理實驗 및 他 數値模型 結果와의 比較를 통하여 본 연구에서 개발한 無限要素에 基礎한 數値模型의 妥當性을 立證하였다. 또한 解析의 效率性과 精度에 直接的으로 影響을 주는 無限要素의 位置決定에 대한 數値實驗도 수행하였다.

1. INTRODUCTION

It has been the case that the site selection of new industrial harbors are mainly determined by the economic situation of the nearby industrial complexes. Accordingly, the harbors can not often find naturally well protected sites for their constructions, and some artificial structures are normally installed to protect harbors from waves. The cargo handling works in the harbors are significantly affected by the degree of harbor tranquility. Hence, from the initial design stage of the plane layout of the harbors as well as breakwater systems, the harbor tranqulity should be properly considered and predicted.

The numerical computation of harbor resonance also belongs to the technology of harbor tranquility analysis. There are three types of the numerical solution techniques for analyzing the harbor resonance, i.e., the finite difference method (FDM: Raichlen and Naheer, 1976), the boundary integral equation method (BIEM) or boundary element method (BEM: Lee, 1969), and the finite element method (FEM: Chen, 1984). Especially, BEM (or BIEM) and FEM are frequently adopted by numerous researchers because of their some advantages in use. But the first peak-period of the resonance in harbor can be estimated almost precisely by any method.

*韓國海洋硏究所 海洋工學硏究部 (Ocean Engineering Division, Korea Ocean Research and Development Institute, Ansan P.O. Box 29, Seoul 425-600, Korea)

Although Lee (1975) developed an extended BEM model in which the computational region is divided into several subregions of different water depth, in general, the application of the BEM model is hardly appropriate to the harbor with varying water depth. Therefore, the interests in the alternative approaches based on the finite element technique have been increased considerably.

Application of the finite element method to surface wave problems have been extensively reviewed by Mei (1978) and Zienkiewicz *et al.* (1978). There are mainly four different approaches in treating the radiation condition at infinity, i.e.,

1. Usage of modified radiation boundary condition: direct or modified radiation condition is applied at the finite distance from the source of the disturbances (Bai, 1972; Huang *et al.*, 1985; Sharan, 1986; Bando *et al.*, 1984).

2. Matching analytical boundary series solutions: the computational wave field is divided into two regions. The internal region including harbors, break-waters, and so an, is discretized into conventional finite elements and the external region located at the outside of the internal region is expressed by analytical solutions. Matching conditions are introduced at the interface of two regions (Bai and Yeung, 1974; Chen andd Mei, 1974; Yue *et al.*, 1978; Chen, 1984; Chen, 1986; Jeong, 1991).

3. Matching boundary integral solutions: Green functions are used at the external region instead of the analytical solution (Bai and Yeung, 1974; Zienkiewicz *et al.*, 1977; Taylor and Zietsman, 1981).

4. Usage of infinite elements: external region is modeled by infinite elments (Bettess and Zienkiewicz, 1977; Zienkiewicz *et al.*, 1985; Lau and Ji, 1989; Chen, 1990; Park *et al.*, 1991; Park *et al.*, 1992).

In this study, the concept of the infinite element has been adopted.

Bettess and Zienkiewicz (1977) firstly applied an infinite element with exponential decay to the horizontal plane problems of surface waves. Later, Zienkiewicz *et al.* (1985) presented a new infinite element with $r^{-1/2}$ decay. It was reported that this element gives more accurate results than the infinite element with exponential decay and any boundary elements. Recently, Chen (19[illegible]) suggested a new infinite element with shape functions derived from the asymptotic behavior of the scattered waves at infinity. It was shown that the element gives fairly good results compared with the analytical solutions and experimental data. However, he did not discuss the proper location of the interface between the inner and outer regions for obtaining appropriate solutions. The location, directly dependent on the incident wave conditions, can significantly affect the solution accuracy and efficency.

In this study, an efficient finite element model incorporating the infinite element has been developed for the prediction of wave resonance phenomena in harbors. Based on the linear wave theory, a mild-slope equation is used. A partial reflection boundary conition is introduced to model the energy dissipating effects on the solid boundary. For modeling efficiently the radiation condition at infinity, a new infinite element is developed. The shape function of the infinite element is derived from the asymptotic behaviors of the first kind of the Hankel' s function in the analytical boundary series solutions. For the computational efficiency, the system matrices of the element are constructed by performing the relevant integrations in the infinite direction analytically. The model can be applied to the harbor with an arbitrary interface angle between the left and right side coastal lines in the exterior region. The effect of the angle can not be considered in the existing models i.e., the hybrid element method, the boundary damper and infinite element techniques. The effects of the energy dissipation on the coastal lines in the outer region can be also considered.

To validate the infinite element, numerical analyses are performed for a fully opened rectangular harbor for which the laboratory data (Ippen and Goda, 1963; Lee, 1969) and the results from other numerical techniques are available. Firstly, some numerical experiments are carried out to set up proper criteria related to the distance to the infinite elements from the mouth of the harbor as well as the size of the finite elements. The criteria directly affect the extent of fluid domain discretization and the solution accuracy. Comparisons with the results from the laboratory experiments and other solution

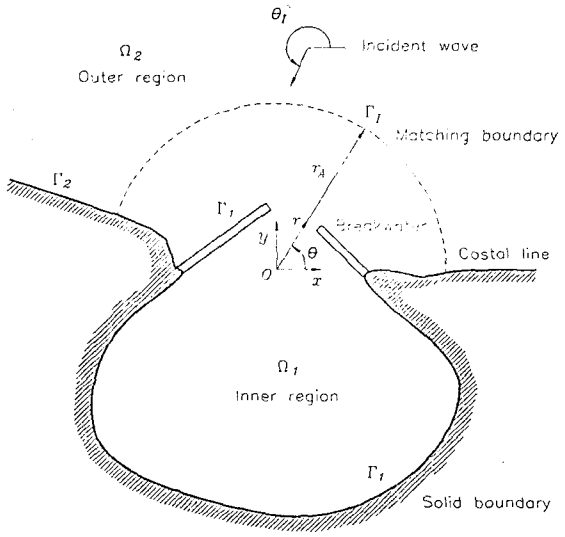

Fig. 1. Definition sketch for the boundary value problem.

methods show that the present model gives fairly good results. Using the appropriately selected criteria, example analyses are also done to investigate the effects of the wave reflecting characteristics on the solid boundary and the effects of the intersection angle between the left and right side coastal lines in the outside of the harbor.

2. THEORETICAL FORMULATION

2.1 Governing Equation

In this study, a Cartesian coordinate system (x, y) and a cylindrical coordinate system (r, θ) are employed with r measured radially from the origin of the Cartesian coordinate system, and θ from the positive x-axis as shown in Fig. 1. The fluid is assumed to be incompressible and inviscid, and the flow is irrotational. A regular wave train is considered, and the wave height is also assumed to be sufficiently small for linear wave theory to be applied.

For the computational efficiency, the wave field is divided into two regions, i.e., inner region Ω_1 inside of the harbor and surrounding area and outer region Ω_2 outside of the inner region. In the outer region, Ω_2, the depth of water is assumed to be constant in the radial direction, but the depth in the circum-ferential direction is varied with that of the interface between the inner and outer regions, Γ_I. In both of inner and outer regions, the wave potential can be expressed as the combination of incident wave potential ϕ_I and scattered wave potential ϕ_S. In the inner region, Ω_1, both wave potentials are not given explicitly, hence their sum ϕ_1 is taken to be unknown, i.e., $\phi_1=\phi_S+\phi_I$. In the outer region, Ω_2, however, the unknown ϕ_2 is taken to be the scattered wave potential, i.e., $\phi_2=\phi_S$ since the incident wave potential, ϕ_I, is assumed to be known.

Then, the monochromatic and simple-time harmonic waves propagating over a mildly sloped sea bed with variable depths in both regions can be described as follows (Berkhoff, 1976; Chen, 1984).

$$\nabla\cdot(CC_g\nabla\phi_i)+\frac{C_g}{C}\omega^2\phi_i=0 \quad \text{in } \Omega_i \tag{1}$$

in which $\nabla=\partial(\cdot)/\partial x\ \vec{i}+\partial(\cdot)/\partial y\ \vec{j}$, $\vec{i}$ and $\vec{j}$ are unit vectors in the direction of x and y, respectively, C is the celerity, C_g is the group veloity, w is the angular frequency, and $\phi(x, y)$ is the two-dimensional spatial complex of veloity potential. Wave celerity, C, and group velocity, C_g, are given as

$$C=\sqrt{\frac{g}{k}\tanh kh} \tag{2}$$

$$C_g=\frac{C}{2}\left[1+\frac{2kh}{\sinh 2kh}\right] \tag{3}$$

in which $h(x, y)$ is the water depth and k is the wave number.

2.2 Boundary Conditions

Coastal boundaries such as slanted coastal lines and breakwaters generally act as wave energy absorbers. To consider the effect of wave absorbing, the absorbing boundary condition is introduced along the solid boundaries, which was developed by Mei and Chen (1975) as a function of an empirical reflection coefficient, K_r normal to the solid boundaries. The boundary condition is represented as

$$\frac{\partial\phi_1}{\partial n}=\alpha\phi_1 \quad \text{on } \Gamma_1 \tag{4}$$

$$\frac{\partial(\phi_2+\phi_I)}{\partial n}=\alpha(\phi_2+\phi_I) \quad \text{on } \Gamma_2 \tag{5}$$

in which n is outward normal to the solid boundary, and α is expressed as

$$\alpha = ik\frac{1-K_r}{1+K_r} \tag{6}$$

Reflection coefficient, K_r, generally depends on the wave frequency and its amplitude, and characteristics of the solid boundary.

The matching boundary condition on the interface between the inner and outer regions, Γ_I, can be expressed as

$$\phi_1 = \phi_2 + \phi_I \text{ or } \phi_2 = \phi_1 - \phi_I \tag{7}$$

$$\frac{\partial \phi_1}{\partial n} = -\frac{\partial(\phi_2+\phi_I)}{\partial n} \text{ or } \frac{\partial \phi_2}{\partial n} = -\frac{\partial(\phi_1-\phi_I)}{\partial n} \tag{8}$$

The scattered wave potential, ϕ_S, in the outer region must satisfy the Sommerfeld radiation condition at infinity (Sommerfeld, 1949).

$$\lim_{r\to\infty} \sqrt{r}\left(\frac{\partial \phi_S}{\partial r} - ik\phi_S\right) = 0 \tag{9}$$

The incident wave potential, ϕ_I, is given as

$$\phi_I = -\frac{ig\zeta_a}{\omega} e^{ikr\cos(\theta-\theta_I)} \tag{10}$$

in which ζ_a is the amplitude of incident wave and θ_I is the attack angle of incident wave.

3. FINITE ELEMENT FORMULATION

3.1 Discretization of Fluid Domain

For the convenience of the finite element formulations, two coordinate systems are used as shown in Fig. 1, that is the Cartesian coordinate for inner region and the cylindrical coordinate for outer region.

To discretize the fluid domain in the standard finite element manner, it is necessary to describe the unknown potential, ϕ_i, in terms of the nodal potential vector, $\{\phi_i^e\}$, for an element (e), and the prescribed shape function vector, $\{N\}$, as follows.

$$\phi_i = \{N\}^T\{\phi_i^e\} \tag{11}$$

The subscript i in equation (11) denotes the inner region for $i=1$ and the outer region for $i=2$.

Using Galerkin's techn.q ie boun y value problem can be re-formulated as integral equations. The element contribution to the system equation can be obtained as

$$\{R^e\} = -\int_{\Omega_i^e}\{N\}\left[\nabla\cdot(CC_g\nabla\phi_i) + \frac{C_g}{C}\omega^2\phi_i\right]d\Omega_i^e \tag{12}$$

in which $\{N\}$ is the vector of element shape functions. Using the technique of integration by parts and Eqs. (4), (5), (7), (8), and (11), the system equations can be obtained as following simultaneous equations:

$$\sum_e([K^e_{\Omega_i}]\{\phi^e\} + [K^e_{\Gamma_i}]\{\phi^e\} + \{F^e_{\Gamma_i}\} - \{F^e_{\Gamma_{Ii}}\}) = \{0\} \tag{13}$$

in which $[K^e_{\Omega_i}]$, $[K^e_{\Gamma_i}]$, $\{F^e_{\Gamma_i}\}$, and $\{F^e_{\Gamma_{Ii}}\}$ are the element system matrices given by

for inner region:

$$[K^e_{\Omega_1}] = \int_{\Omega_1^e}\left[CC_g\left(\left\{\frac{\partial N}{\partial x}\right\}\left\{\frac{\partial N}{\partial x}\right\}^T + \left\{\frac{\partial N}{\partial y}\right\}\left\{\frac{\partial N}{\partial y}\right\}^T\right) - \frac{C_g}{C}\omega^2\{N\}\{N\}^T\right]d\Omega_1^e \tag{14}$$

$$[K^e_{\Gamma_1}] = \int_{\Gamma_1^e} CC_g\alpha\{N\}\{N\}^T\, d\Gamma_1^e \tag{15}$$

$$\{F^e_{\Gamma_1}\} = \{0\} \tag{16}$$

$$\{F^e_{\Gamma_{I1}}\}\int_{\Gamma_I^e} CC_g\frac{\partial(\phi_2+\phi_I)}{\partial n}\{N\}d\Gamma_I^e \tag{17}$$

for outer region:

$$[K^e_{\Omega_2}] = \int_{\Omega_2^e}\left[CC_g\left(\left\{\frac{\partial N}{\partial r}\right\}\left\{\frac{\partial N}{\partial r}\right\}^T + \frac{1}{r^2}\left\{\frac{\partial N}{\partial \theta}\right\}\left\{\frac{\partial N}{\partial \theta}\right\}^T\right) - \frac{C_g}{C}\omega^2\{N\}\{N\}^T\right]d\Omega_2^e \tag{18}$$

$$[K^e_{\Gamma_2}] = \int_{\Gamma_2^e} CC_g\alpha\{N\}\{N\}^T\, d\Gamma_2^e \tag{19}$$

$$\{F^e_{\Gamma_2}\} = \int_{\Gamma_2^e} CC_g\left(\alpha\phi_I - \frac{\partial\phi_I}{\partial n}\right)\{N\}d\Gamma_2^e \tag{20}$$

$$\{F^e_{\Gamma_{I2}}\}\int_{\Gamma_I^e} CC_g\frac{\partial(\phi_1-\phi_I)}{\partial n}\{N\}d\Gamma_I^e \tag{21}$$

3.2 Finite and Infinite Elements

The inner region, Ω_1, is modeled by using two isoparametric elements, i.e., eight-noded element and three-noded line element as shown in Figs. 2 and 3. The Lagrange polynomials are used for the shape functions of the elements. The eight-noded element

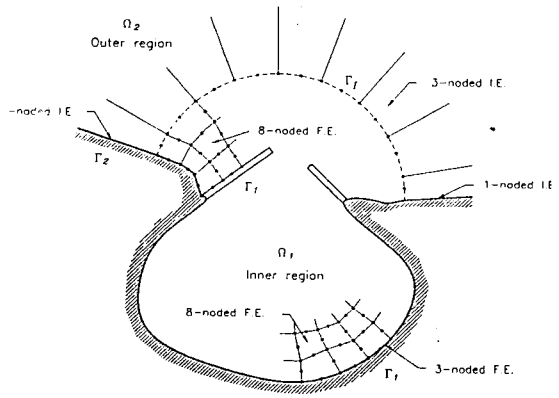

Fig. 2. Discretization of fluid domain.

is used for discretizing the fluid domain whereas the three-noded element in used for modeling the absorbing boundary conditions. The integrations of quations (14)-(17) are made using Gauss-Legendre quadrature (Carnahan *et al.*, 1969), and the system matrices are finally constructed.

In order to model efficiently the radiation condition at infinity, and to consider properly the absorption of wave energy along the coastal lines of the outer region, two infinite elements are developd, i.e., three-noded element and one-noded line lement as shown in Fig. 2 and 4. The three-noded infinite element is used for disscretizing the fluid domain in the outer region, and the one-noded element is used for modeling the energy dissipation effects along the coastal lines in the outer region. The shape functions of the elements are derived from the analytical boundary series solutions given by for three-noded infinite element ($0 \leq \xi \leq \infty$, $-1 \leq \eta \leq 1$):

$$\{N\} = N_A(\xi)\{N_\theta(\eta)\} \tag{22}$$

for one-noded infinite element ($0 \leq \xi \leq \infty$):

$$\{N\} = N_A(\xi) \tag{23}$$

in which $\{N_\theta(\eta)\}$ is the Lagrange shape functions, and $N_A(\xi)$ is the shape function in the radial direction given by

$$N_A(\xi) = \frac{\sqrt{r_A}}{\sqrt{\xi + r_A}} e^{(ik-\varepsilon)\xi} \tag{24}$$

in which ε is the artificial damping parameter ($\varepsilon <$

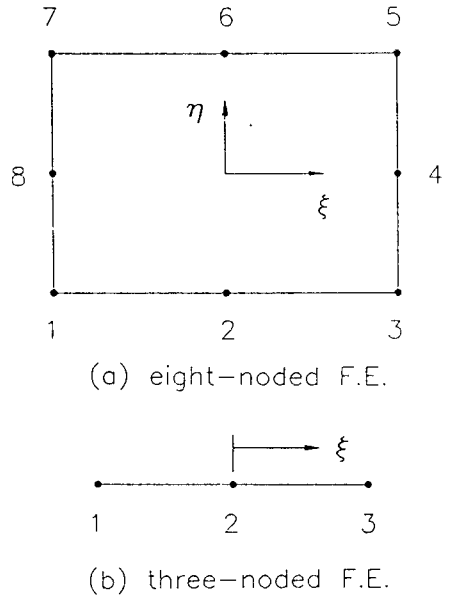

Fig. 3. Coordinate systems for finite elements.

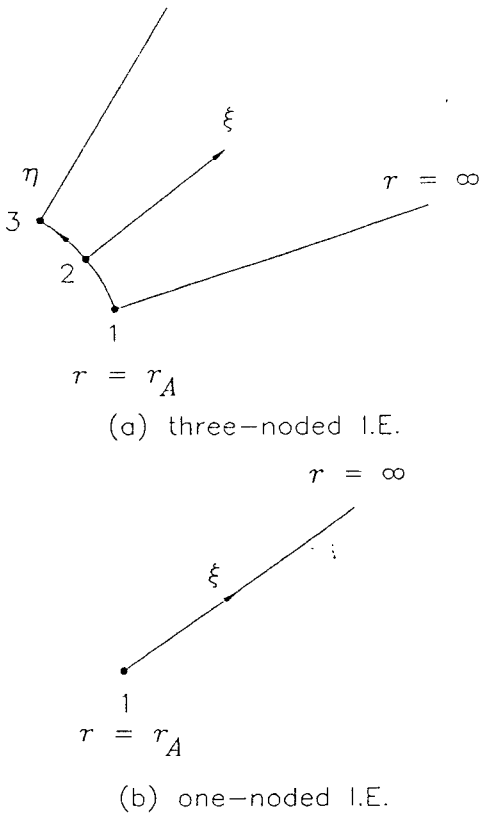

Fig. 4. Coordinate systems for infinite elements.

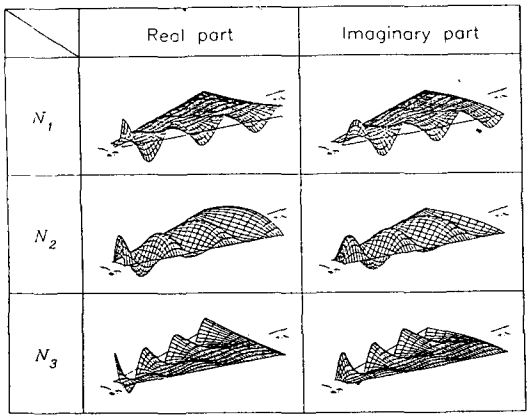

Fig. 5. Shape functions for the three-noded infinite element.

k), and r_A is the distance to the infinite elements from the origin as shown in Fig. 1. The artificial damping parameter, ε, has been introduced, to make the integration in Eq. (18) in the radial direction bounded. After the integration is completed analytically, the value of ε is taken to be zero.

The shape function, $N_i(\xi)$, in the radial direction, except for the artificial damping parameter, have been derived from the asymptotic expression for the first kind of Hankel's function in the analytical boundary series solutions such as

$$\phi_S \propto \frac{1}{\sqrt{r}} e^{ikr} \tag{25}$$

It is noted that the corresponding shape function satisfies the radiation condition at infinity. In Fig. 5, the shape functions for the three-noded infinite element as given in Eq. (22) are presented in real coordinate system.

Then, the system matrices can be constructed using Eqs. (18)-(21) as

$$[K^e_{\Omega 2}] = A_1[K_{\theta\theta}] + A_2[K_{\theta'\theta'}] - A_3[\bar{K}_{\theta\theta}] \tag{26}$$

$$[K^e_{\Gamma 2}] = A_4 CC_g \tag{27}$$

$$\{F^e_{\Gamma 2}\} = A_5 CC_g \frac{ig\zeta_a}{\omega}(ik(n_x\cos\theta_I + n_y\sin\theta_I) - \alpha) \tag{28}$$

in which n_x and n_y are the x and y components of the outward normal vector to the Γ_2, and A_i's are the complex valued coefficients resulting from the integration of Eqs. (18)-(20) in the infinite direction (see Appendix), and $[K_{\theta\theta}]$, $[\bar{K}_{\theta\theta}]$, $[K_{\theta'\theta'}]$ are defined as

$$[K_{\theta\theta}] = \int_{\theta^e} CC_g\{N_\theta\}\{N_\theta\}^T \, d\theta^e \tag{29}$$

$$[\bar{K}_{\theta\theta}] = \int_{\theta^e} \frac{C_g}{C}\omega^2\{N_\theta\}\{N_\theta\}^T \, d\theta^e \tag{30}$$

$$[K_{\theta'\theta'}] = \int_{\theta^e} CC_g\left\{\frac{\partial N_\theta}{\partial\theta}\right\}\left\{\frac{\partial N_\theta}{\partial\theta}\right\}^T d\theta^e \tag{31}$$

Gauss-Legendre quadrature is used for the integration in the above equations in the θ-direction.

3.3 Matching the Inner and Outer Regions

The total velocity potential is unknown in the inner region while the scattered potential is unknown in the outer region. Therefore, it is necessary to ensure matching the unknown velocity potentials in the inner and outer regions.

Using the matching boundary conditions in Eqs. (7) and (8), the total system matrices can be assembled as

$$\sum_e([K^e_\Omega]\{\phi^e\} + [K^e_\Gamma]\{\phi^e\} + F^e_\Gamma\} + \{F^e_{\Gamma_I}\}) = \{0\} \tag{32}$$

in which

$$[K^e_\Omega] = [K^e_{\Omega_1}] + [K^e_{\Omega_2}] \tag{33}$$

$$[K^e_\Gamma] = [K^e_{\Gamma_1}] + [K^e_{\Gamma_2}] \tag{34}$$

$$\{F^e_\Gamma\} = \{F^e_{\Gamma_2}\} \tag{35}$$

$$\{F^e_{\Gamma_I}\} = -\int_{\Gamma_I^e} CC_g\frac{\partial\Phi}{\partial n}\{N\}d\Gamma^e_I - ([K^e_{\Omega_2}] + [K^e_{\Omega_2}])\ \{\phi^e_I\} \tag{36}$$

and $\{\phi^e_I\}$ is the vector of the incident wave potential corresponding to nodal points.

4. NUMERICAL RESULTS AND DISCUSSIONS

A numerical model is applied to the rectangular harbor to demonstrate its validity. The accuracy and efficiency of the model depend on two major factors, that is, the location of the interface between the inner and outer regions, and the size of the finite elements. Firstly, numerical experiments are

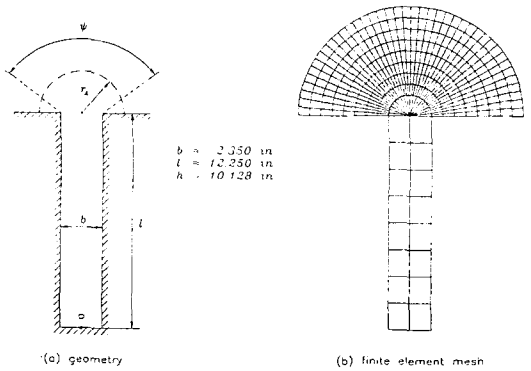

Fig. 6. Geometry of a model harbor and finite element mesh.

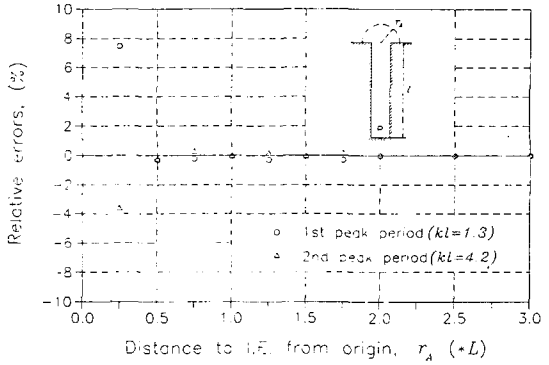

Fig. 7. Relative errors with varying r_A compared with the results for $r_A=3L$.

performed to determine the appropriate criteria of both factors. Then, using these criteria, example analyses are carried out for the harbor varying the reflection characteristics of the solid boundary, Γ_1 and the intersection angle, ψ, between the left and right sides of coastal lines in the outer region.

4.1 Model Harbor

A fully-opened rectangular harbor is adopted as a model harbor. Since the experimental data (Ippen and Goda, 1963; Lee, 1969) and the results from the other numerical techniques are available, the harbor is frequently used as a reference harbor in order to verify numerical models. The geometry of the harbor is presented in Fig. 6(a). The harbor width is 2.38 inches, the length of harbor is 12.25 inches, and the water depth is constant of 10.128 inches in the entire fluid domain. The point, $P(0.0, -12.25)$ is a reference point for comparisons of the wave amplification ratios. An example of the finite element mesh used for numerical experiments is presented in Fig. 6(b).

4.2 Location of Infinite Element

The analysis is performed for various locations of the infinite elements from $r_A=0.25\times L$ to $r_A=3.0\times L$ in which L is incident wave length. Two wave conditions (the first and the second resonance conditions of the harbor) are considered. The amplification ratios of wave height are calculated and compared at the point P. The experimntal results are presented in Fig. 7, which are relative errors compared to the results obtained from the case with $r_A=3.0\times L$. It is found in this figure that the suitable location of the infinite element may be determined as 0.5 times the incident wave length from the mouth of the harbor ($r_A=0.5\times L$).

4.3 Effects of Finite Element Size

To investigate the size effects of the finite element, the numerical analysis is carried out using six different size conditions, i.e., 1/4, 1/8, 1/12, 1/16, 1/20, and 1/24 of the wave length, L. The infinite elements are fixed at $r_A=0.5\times L$. The amplification ratio at the point P is also used as a check point. The relative errors of each element size with respect to $1/24\times L$ are shown in Fig. 8. It is found that the results rapidly converged with the increase of the number of finite elements per wave length. It can be also observed that finer meshes are required for the case of longer period wave condition. In general, a criterion such that the size of the finite element is less than the 0.25 times the incident wave length has been accepted for the case of quadratic elements used here. However, the present results indicate that the criterion may not be adequate. It should be noted that the phenomenon is based on the fact that the wave lengths used here are very long compared to the size of the harbor. The criterion above may be still available for the case of short period wave conditions.

4.4 Example Analysis

From the numerical experiment above, the proper

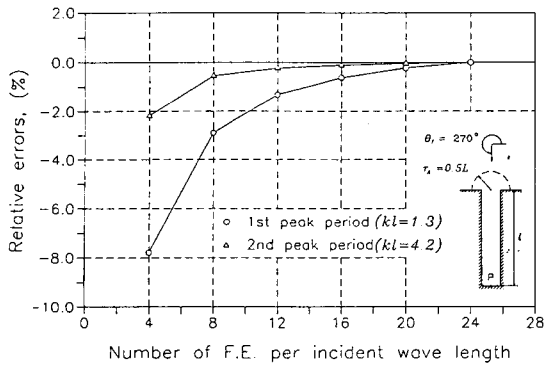

Fig. 8. Relative errors with the number of finite elements per wave length (L) varied.

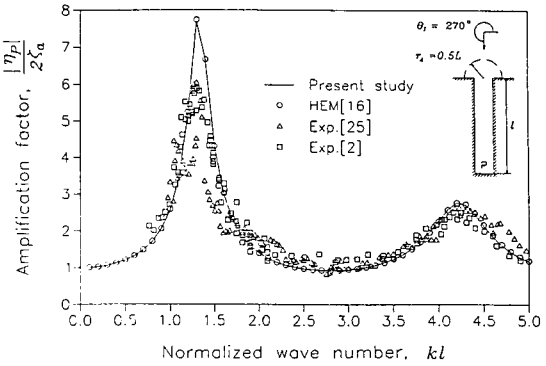

Fig. 9. Comparison of amplification ratios between the numerical and exprimental results.

location of the infinite element is set as $r_A=0.5\times L$ while the finite element size is fixed to $1/24\times L$. Using the criteria, example analyses are carried out for the model harbor with following conditions:

1. Different reflection characteristics on the solid boundary
2. Different attack angle of the incident wave, θ_I
3. Different intersection angle, ψ, between the left and right side coastal lines in the outer region.

4.4.1 Effects of Reflection Characteristics

In numerical models, it is commonly assumed that there is no friction on side walls and bottom of wave basin, and full reflection on the solid boundary. In real case, it is however impossible to complete an experiment without the effect of wave energy dissipation. To obtain more accurate results, that effect must be considered properly in the numerical model. If not, the estimations may be quite over-predicted, particularly when the resonance conditions are met.

Fig. 9 shows the comparison of the results of wave amplification ratios at point P for long-period wave conditions. In the figure, the solid line denotes the present results for the case of full reflection, the rectangular symbols denote the computational results by Hybrid Element Method (Jeong, 1991). The circle and triangular symbols indicate the experimental results by Ippen and Goda (1963) and Lee (1969), respectively. Both numerical results show good agreements with the exprimental results, except for the slight over-estimations around the first reso-

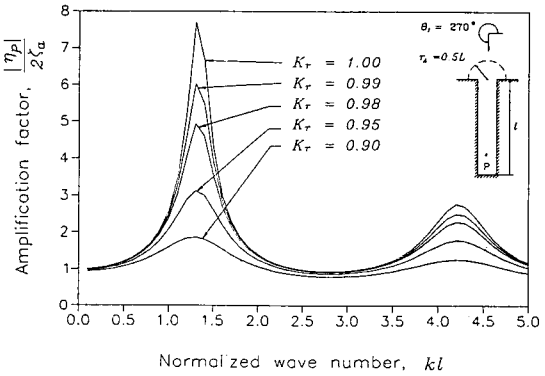

Fig. 10 Amplificaton ratios for various values of reflection coefficient, K_r, on the solid boundary.

nance condition.

Fig. 10 shows the variations of the amplification ratios at the point P with varying reflection cofficients in the inner region. In this figure, it is known that the amplification ratios are very sensitive to the reflection coefficient in case of long-period waves, particularly at the wave resonance conditions. The results for the case of $K_r=0.99$ are quite well compared with the experimntal results in Fig. 9 especially at the first peak period.

4.4.2 Effects of Attack Angles of the Incident Wave

Fig. 11 presents the results for three different attack angle of incident waves, i.e., $\psi=270°$, 240°, 210°. The results indicate that the wave attack angle, ψ, does not much effect on the harbor resonance phenomena. However, the effect may appear significantly for the case of short-period wave conditions.

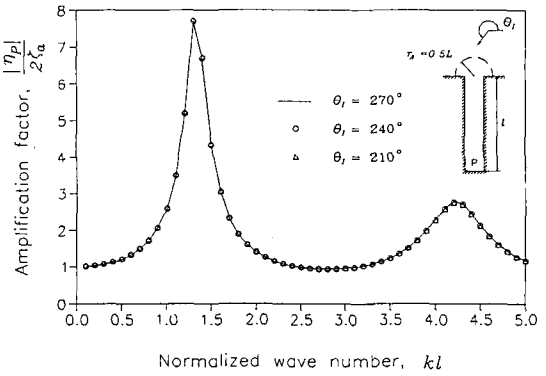

Fig. 11. Amplification ratios for three different angles of wave attack, θ_I.

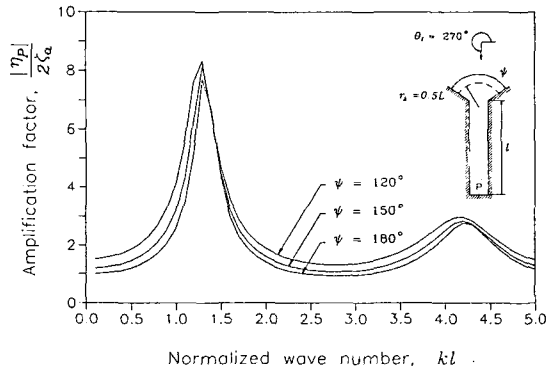

Fig. 12. Amplification ratios for three different intersection angles, ψ, between the left and right sides of coastal lines in the outer region.

4.4.3 Effects of Intersection Angles, ψ

The present algorithm can be applied to the case of the arbitrary intersection angle, ψ, between the left and right sides of coastal lines in the outer region (see Fig. 6(a)). Fig. 12 shows the results for three different intersection angles. The results indicate that the amplification ratios increase as the intersection angle, ψ, decreases, but the resonance frequencies are hardly affected.

5. CONCLUSIONS

In this study, an efficient finite element model incorporating the infinite element has been developed for the prediction of the harbor resonance phenomena. The model can be applied to the harbor with an arbitrary intersection angle between the left and right sies of coastal lines in the outer region. To model the radiation condition at infinity, an infinite element is developed. The shape function of the infinite element is derived from the asymptotic behaviors of the progressive wave components in the analytical boundary series solutions. For the computational efficiency, the system matrices of the element are constructed by performing the integration in the infinite direction analytically.

The major conclusions obtained by the present model are summarized as follows:

1. The present finite element model incorporating infinite elements for modeling radiation condition gives fairly nice results well agreed with the experimental data and those obtained by other available solution methods.

2. The extent of the enlargement of the inner domain in directly dependent on the incident wave length, and its suitable location is determined as 0.5 times the incident wave length from the mouth of the harbor (r_A=0.5×L).

3. Although the quardratic elements are used, the size of the finite element should be much less than 0.25 times the incident wave length to obtain reasonable results, particularly for long-period wave conditions.

4. The wave amplification ratios are significantly affected by the variation of reflection characteristics on the solid boundary, particularly around the resonance conditions.

5. The example analysis with various intersection angle, ψ, between the left and right sides of coastal lines in the outer region indicate that the amplification ratios increase as the intersection angle, ψ, decreases, but the resonance frequencies are hardly affected.

ACKNOWLEDGEMENTS

Partial support for this research was provided by the Korea Ocean Research and Development Institute through Grant BSPE 00401.

APPENDIX: DETERMINATION OF A_i's

In equations (26)-(28), A_i's are the complex valued

coefficients associated with the integration in the radial direction as follows.

$$A_1=\int_0^\infty r_A\left(ik-\varepsilon-\frac{1}{2(\xi+r_A)}\right)^2 e^{2ik\xi-2\varepsilon\xi}\,d\xi$$

$$A_2=\int_0^\infty r_A\frac{1}{(\xi+r_A)^2}e^{2ik\xi-2\varepsilon\xi}\,d\xi$$

$$A_3=\int_0^\infty r_A e^{2ik\xi-2\varepsilon\xi}\,d\xi$$

$$A_4=\int_0^\infty \frac{r_A}{\xi+r_A}e^{2ik\xi-2\varepsilon\xi}\,d\xi$$

$$A_5=\int_0^\infty \sqrt{\frac{r_A}{\xi+r_A}}\,e^{ik\xi+(\xi+r_A)\cos(\theta-\theta_I)-\varepsilon\xi}\,d\xi$$

After integrating the above equations with respect to ξ from 0 to infinity, and taking $\varepsilon=0$, the A_i's can be obtained as function of k and r_A, which are given by

$$A_1=\frac{1}{4}-\frac{ikr_A}{2}[1-e^{-2ikr_A}(c_i(2kr_A)+is_i(2kr_A))]$$

$$A_2=1-2ikr_Ae^{-ikr_A}[c_i(2kr_A)+is_i(2kr_A)]$$

$$A_3=\frac{ir_A}{2k}$$

$$A_4=-r_Ae^{-2ikr_A}\{c_i(2kr_A)+is_i(2kr_A)\}$$

$$A_5=\sqrt{r_Ae^{-ikr_A}}\sqrt{\frac{\pi}{-ik(1+\cos(\theta-\theta_I))}}$$
$$[1-\Phi(\sqrt{-ikr_A(1+\cos(\theta-\theta_I))})]$$

in which $c_i(\cdot)$ and $s_i(\cdot)$ are cosine and sine integral functions defined as (Gradshteyn and Ryzhik, 1980)

$$c_i(x)=-\int_x^\infty\frac{\cos t}{t}dt=\gamma+\ln(x)+\int_0^x\frac{\cos t-1}{t}\,dt$$

$$s_i(x)=-\int_x^\infty\frac{\cos t}{t}dt=-\frac{\pi}{2}+\int_0^x\frac{\sin t}{t}dt$$

and, $\Phi(\cdot)$ is error function defined as

$$\Phi(x)=\frac{2}{\sqrt{\pi}}\int_0^x e^{-t^2}dt$$

In the above equations, γ is the Euler's constant ($=0.5772156649$) and $\ln(\cdot)$ is the natural logarithm. These integral values are obtained by using IBM application problem (1970) (SSP: Scientific Subroutine Package) with slight modifications.

REFERENCES

Bai, K.J., 1972. A variational method in potential flows with a free surface, *Report No. NA72-2*, College of Engrg, Univ. of California, Berkeley.

Bai, K.J. and Yeung, R.W., 1974. Numerical solutions of free-surface flow problems, *Proc. of 10th Symp. in Naval Hydrodynamics*, Office of Naval Research, pp. 609-647.

Bando, K., Bettess, P. and Emoson, C., 1984. The effctiveness of dampers for the analysis of exterior scalar wave diffraction by cylinders and ellipsoids, *Int. J. Num. Meth. in Fluids*, Vol. 4, pp. 599-617.

Berkhoff, J.C.W., 1976. Mathematical model for simple harmonic linear water waves: Wave diffraction and refraction, *Report No. 163.*, Delft Hydraulic Laboratory.

Carnahan, B., Luther, H.A. and Wilkes, J.O., 1969. *Applied Numerical Methods*, John Wiley & Sons, Inc.

Bettess, P. and Zienkiewicz, O.C., 1977. Diffraction and refraction of surface waves using finite and infinite elements, *Int. J. Numer. Meth. in Engrg.*, 11, pp. 1271-1290.

Chen, H.S., 1984. Hybrid element modelling of harbor resonance, *4th Int. Conf. on Applied Numerical Modelling.*

Chen, H.S., 1986. Effects of bottom friction and boundary absorption on water wave scattering, *Applid Ocean Res.*, 8, pp. 99-104.

Chen, H.S., 1990. Infinite elements for water wave radiation and scattering, *Int. J. Numer. Meth. in Fluids*, 11, pp. 555-569.

Chen, H.S. and Mei, C.C., 1974. Oscillations and wave forces in an offshore harbor. *Report No. 190*, Ralph M. Parsons Lab., M.I.T.

Gradshteyn, I.S. and Ryzhik, I.M., 1980. *Table of Integral, Series, and Products*, Academic Press, New York.

Huang, M.C., Leonard, J.W. and Hudspeth, R.T., 1985. Wave inteference effects by finite element method, *J. of Waterway, Port, Coastal and Ocean Division, ASCE*, 111(1), pp. 1-17.

IBM application program. 1970. *System/360 Scientific Pakage (SSP)*, Version III, Programmer's Mannual, International Business Machines Corporation.

Ippen, A.T. and Goda, Y., 1963. Wave induced oscillation in harbor: Thee solution for a rectangular harbor connected to the open-sea, *Report No. 59*, Hydrodynamics Laboratory, M.I.T.

Jeong, W-M., 1991. Analysis of wave agitations in harbours by hybrid element method, MSc Thesis, Myong-Ji Univ.

Lau, S.L. and Ji, Z., 1989. An efficient 3-D infinite element for water wave diffraction problems, *Int. J. Numer. Meth. in Engrg.*, **28**, pp. 1371-1387.

Lee, J.J., 1969. Wave induced oscillations in harbors of arbitrary shape, Ph. D. Thesis, California Institute of Technology.

Lee, J.J., 1975. Oscilations in harbors with connected basins, *Proc. Civil Eng. in Oceans*, I, pp. 632-645.

Mei, C.C., 1978. Numerical methods in water-wave diffraction and radiation, *Annual Review Fluid Mechanics*, 10,

pp. 393-416.

Mei, C.C. and Chen, H.S., 1975. Hybrid-element method for water wave, *Proc. of Symp. on Modeling Tech.* San Fransisco.

Park, W-S., Yun, C-B. and Pyun, C-K., 1991. Infinite elements for evaluation of hydrodynamics forces on offshore structures, *Computers and Structures*, **40**(4), pp. 837-847.

Park, W-S., Yun, C-B. and Pyun, C-K., 1992. Infinite elements for three-dimensional wave-structure interaction problems, *Engineering Structures*, **14**(5), pp. 335-346.

Raichlen, F. and Naheer, E., 1976. Wave induced oscillations of harbor with variable depth, *Proc. 15th ICCE*, pp. 3536-3556.

Sharan, S.K., 1986. Modelling of radiation damping in fluids by finite elements, *Int. J. Numer. Meth. in Engrg.*, **23**, pp. 945-957.

Sommerfeld, A., 1949. *Partial Differential Equations in Physics*, Academic Press, New York.

Taylor, R.E. and Zietsman, J., 1981. A comparison of localized finite element formulations for two-dimensional wave diffraction and radiation problems, *Int. J. Numer. Meth. in Engrg.* **17**, pp. 1355-1384.

Yue, D.K.P., Chen, H.S. and Mei, C.C., 1978. A hybrid element method for diffraction of water waves by three-dimensional bodies, *Int. J. Numer. Meth. in Engrg.*, **12**, pp. 245-266.

Zienkiewicz, O.C., Bettess, P. and Kelly, D.W., 1978. The finite element method for determining fluid loading on rigid structures, two- and three-dimensional formulations, *Numer. Meth. in Offshore Engrg.*, Zienkiewicz, O.C. *et al.*, eds, Wiley, Chicheser, England, pp. 141-183.

Zienkiewicz, O.C., Emson, C. and Bettess, P., 1985. A novel boundary infinite element, *Int. J. Numer. Meth. in Engrg.*, **19**, pp. 393-404.

Zienkiewicz, O.C., Kelly, D.W. and Bettess, P., 1977. The coupling of the finite element method and boundary solution procedures, *Int. J. Numer. Meth. in Engrg.*, **11**, pp. 355-375.